Journal of Molecular Graphics and Modelling 28 (2010) 728–734

Contents lists available at ScienceDirect

Journal of Molecular Graphics and Modelling

journal homepage: www.elsevier.com/locate/JMGM

Role of Arg301 in substrate orientation and catalysis in subsite 2 of D-alanine:D-alanine (D-lactate) ligase from *Leuconostoc mesenteroides*: A molecular docking study

Francis C. Neuhaus *

Department of Biochemistry, Molecular and Cellular Biology, 2205 Tech Drive, Northwestern University, Evanston, IL 60208-3500, USA

ARTICLE INFO

Article history:
Received 9 November 2009
Accepted 22 January 2010
Available online 1 February 2010

Keywords:
Molecular docking
D-Alanine:D-alanine (D-lactate) ligase (ADP)
AutoDock 4
D-Lactate
Vancomycin resistance

ABSTRACT

D-Alanine:D-alanine (D-lactate) ligase (ADP) from *Leuconostoc mesenteroides* synthesizes the depsipeptide, D-alanyl-D-lactate, in addition to D-alanyl-D-alanine, when D-alanine and D-lactate are incubated simultaneously. The depsipeptide is responsible for the intrinsic resistance of this organism to vancomycin. The orientations of D-lactate and D-alanine in subsite 2 of the ligase that result in both nucleophile generation and subsequent attack on the electrophilic center of D-alanyl phosphate in subsite 1 are not known. A molecular docking study using AutoDock 4 suggests a role for Arg301 in determining these orientations of acceptor substrate in subsite 2 for both nucleophile generation and subsequent attack on the phosphate intermediate.

With D-lactate a bifurcated H-bond from Arg301 to the R–OH of D-lactate may account for its orientation and nucleophile activation. This orientation is observed when the guanidino side chain of this residue is flexible. D-Alanine adopts an orientation that utilizes H-bonding to water 2882 and the D-alanyl phosphate in subsite 1. Both of these orientations provide mechanisms of deprotonation and place the nucleophile within 3.2 Å of the electrophilic carbonyl of the D-alanyl phosphate intermediate for formation of the transition state.

These results suggest that Arg301 has a dual function in a sequential reaction mechanism, i.e. substrate orientation in subsite 2 as well as stabilization of the transition state. In addition, these docking studies provide insights for inhibitor design targeted to this subsite of the ligase.

1. Introduction

D-Alanyl-D-alanine is an essential intermediate in the biosynthesis of peptidoglycan, a major structural polymer of the bacterial cell wall. The synthesis of this dipeptide is catalyzed by D-alanine:D-alanine ligase (ADP) [1–3]. Phylogenetic analyses of this enzyme define five subfamilies [4–6]. One of these, represented by *Leuconostoc mesenteroides*, also utilizes D-lactate as a substrate together with D-alanine in this ligation [7]. Thus, the organism can synthesize cross-linked peptidoglycan using either UDP-MurNAc-L-Ala-D-Glu-L-Lys-D-Ala-D-Ala or UDP-MurNAc-L-Ala-D-Glu-L-Lys-D-Ala-D-lactate [7–9].

Kinetic analyses of the D-alanine:D-alanine ligase family established two subsites in the catalytic center for binding D-alanine [10–12]. Subsite 1 is characterized by both a higher affinity and a higher specificity for D-alanine than subsite 2 [10,13]. For example, with the ligase from *Enterococcus hirae* (formerly *Streptococcus faecalis R* 8043) D-α-amino-*n*-butyrate is a poor substrate for subsite 1 and a good substrate for subsite 2. Simultaneous incubation of these amino acids results in a significant synthesis of the mixed dipeptide (D-ala-D-α-amino-*n*-butyrate) as well as D-ala-D-ala [10]. The ligase from *L. mesenteroides* catalyzes the synthesis of the depsipeptide (D-ala-D-lactate) in addition to D-ala-D-ala when D-alanine and D-lactate are incubated simultaneously [7]. In each of the D-alanine:D-alanine ligases the catalytic events in subsite 1 culminate in the transfer of the γ-phosphoryl of ATP to the carboxyl group of D-alanine with formation of the aminoacyl phosphate intermediate in the presence of Mg^{2+} [12]. The orientations of D-lactate and D-alanine in subsite 2 of the ligase that result in both nucleophile generation and subsequent attack on the electrophilic center of D-alanyl phosphate in subsite 1 are not known.

From a combination of mutagenesis experiments [5,7,14] sequence alignments [4,6,15] and crystallographic studies [15–20] of ligases from a variety of bacteria, many of the amino acid residues that play primary role(s) in subsites 1 and 2 have been defined [14,15,21]. Kuzin et al. [17] established the crystallographic structure of the *L. mesenteroides* ligase with a transition-

* Tel.: +1 847 491 5656; fax: +1 847 467 1380.
E-mail address: f-neuhaus@northwestern.edu.

1093-3263/$ – see front matter © 2010 Elsevier Inc. All rights reserved.
doi:10.1016/j.jmgm.2010.01.010

state analog in the presence of Mg^{2+} and ADP. From this structure amino acid residues in subsite 2 for ligand binding were identified. These include Arg301 located at the interface of the subsites functioning together with Gly322 to form the oxyanion hole for stabilization of the transition-state intermediate. In addition, four other residues in this ligase, Met326, Ser327, Leu328 and Phe261 determine in part the binding specificity of subsite 2 [6,17]. Ideally, one could establish the steric constraints and substrate orientations of D-alanine or D-lactate if it were possible to co-crystallize the ligase with either substrate. Since this has not been feasible, the binding modes and catalytic processes of D-lactate and D-alanine utilization in subsite 2 have not been readily elucidated.

Inhibition of peptidoglycan assembly by vancomycin results from complex formation of this glycopeptide antibiotic with the acyl-D-alanyl-D-alanine of the undecaprenol-diphosphate MurNAc-pentapeptide intermediate [22–24]. This complex prevents further peptidoglycan synthesis and crosslinking. With UDP-MurNAc-tetrapeptide as substrate no inhibition of glycan synthesis by vancomycin is observed [23]. Replacement of the acyl-D-ala-D-ala of UDP-MurNAc-pentapeptide with D-ala-D-lactate yields UDP-MurNAc-tetrapeptide-D-lactate. This analog substrate is effectively utilized for cross-linked peptidoglycan synthesis in the presence of vancomycin and, thus, resistance to the antibiotic results. Vancomycin binds with a greatly reduced affinity (1000-fold) to cell wall intermediates that terminate in acyl-D-ala-D-lactate when compared to acyl-D-ala-D-ala [22]. D-Alanine:D-alanine (D-lactate) ligases from *L. mesenteroides*, lactobacilli, and enterococci (VanA and VanB) that can synthesize D-ala-D-lactate, as well as D-ala-D-ala, are of major interest for their role in determining this resistance phenotype [5,6,17,19,25–28] In addition to the role of this ligase in vancomycin resistance, the enzyme has also been the focus of inhibitor design and screening programs to identify new antibacterial agents [15,29–33]. One of these programs [29] that utilizes AutoDock 4 for virtual screening has identified three promising inhibitors from the National Cancer Institute Diversity Set.

It is the goal of this paper to utilize AutoDock 4 to investigate the docking orientations of D-lactate and D-alanine in subsite 2 of the D-alanine:D-alanine (D-lactate) ligase from *L. mesenteriodes* and to study the role of Arg301 in assisting nucleophile activation in the ligation reaction.

2. Methodology

2.1. Software and PDB files

To examine the substrate orientations of D-alanine and D-lactate in subsite 2 of the ligase, AutoDock 4 and AutoDockTools 4 (ADT) were chosen [34,35]. The choice of AutoDock 4 for these studies was based on selective receptor flexibility in subsite 2 as well as flexible bonds in the ligands, D-alanine and D-lactate. A crystal structure [17] of D-alanine:D-alanine (D-lactate) ligase (ADP) from *L. mesenteroides* (PDB ID: 1EHI) was retrieved from the RCSB Protein Data Bank.

2.2. Ligand and protein files

The ligands, D-lactate, L-lactate, D-alanine and L-alanine, were drawn in ChemDraw and then converted to the AutoDock 4 PDBQT file format using ADT. In the case of alanine the zwitterion was chosen as the ligand [36]. The bonds of lactate (C^{α}–OH and C^{α}–COO^{-}) and of alanine (C^{α}–NH_3^{+} and C^{α}–COO^{-}) were allowed to rotate in the docking studies. This flexibility was also programmed into the PDBQT files with the use of ADT.

The PDB file for the D-alanine:D-alanine ligase contains the coordinates for monomers A and B of the unit cell. Co-crystallization

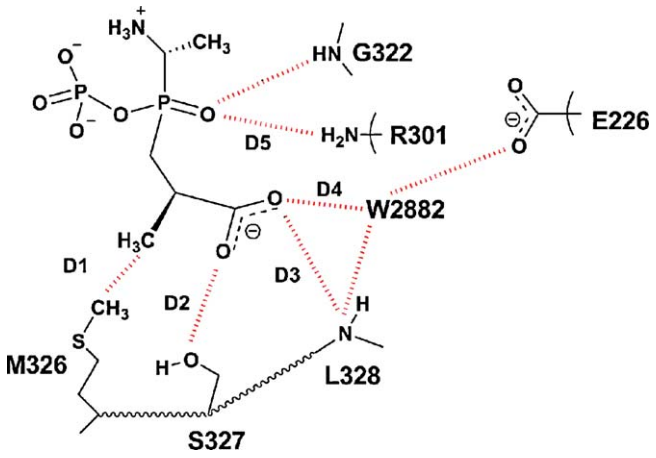

Fig. 1. Schematic identifying the distances of the transition-state analog, phosphoryl-phosphinate **2**, to key residues of the ligase listed in Table 1. The distances, D1–5 are designated. Gly322 and Arg301 determine the oxyanion hole (adapted from Ref. [17]). (For interpretation of the references to color in this figure legend, the reader is referred to the web version of the article.)

of the protein with ATP and 1(*S*)-amino-ethyl (2-carboxy-2(*R*)-methyl-1-ethyl) phosphinic acid **1** resulted with the transfer of the γ-phosphoryl of ATP in monomer A to the phosphinic acid **1** yielding the transition-state analog, phosphorylated phosphinate **2** (Fig. 1). Monomer A exists in a closed form restricting access to the catalytic center while monomer B, which lacks the phosphorylated phosphinate **2**, is in an open form [17]. Monomer A was energy minimized in Swiss-PdbViewer [37] before the following changes were made. Three modifications were made to the PDB file of monomer A. First, to provide access to subsite 2, the Ω-loop (residues 247–267) and the serine–serine loop (residues 185–188) were removed. Second, Kuzin et al. [17] observed that a water bridges between the carboxylate of phosphorylated phosphinate **2** and the backbone amide of Leu328 (Fig. 1). After removal of monomer B from the PDB file the bridging water is renumbered 2882. All other water molecules have been removed for these studies. Third, docking in subsite 2 utilizes enzyme-bound D-alanyl phosphate in subsite 1. To incorporate this structure, the phosphorylated phosphinate **2** in the PDB file was replaced with D-alanyl phosphate. In addition, the molecular charge on each of the two Mg^{2+} cations was varied between +0.8 and +1.2 and set at +1 according to Chen et al. [38] The molecular charges on ADP were calculated by the method of Gasteiger and Marsili [39]. Each of these modifications and calculations is essential for the docking studies in subsite 2. Using monomer A has the advantage of preserving the catalytic architecture of the amino acid side residues that determine subsites 1 and 2.

2.3. Docking protocol

The basic docking protocol was adopted using the default settings provided by ADT [40]. The protein structure and the flexible Arg301 guanidino group were converted to PDBQT format in ADT. The Lamarckian Genetic Algorithm was used with a population size of 150 dockings. Five million energy evaluations were used in most dockings except where noted. All other parameters, e.g. crossover rate and mutation rate, were run with default settings. The grid size for specifying the search space was set at $21 \times 21 \times 21$ centered in subsite 2 with a default grid point spacing of 0.375 Å. The force field for AutoDock 4 was calibrated with a set of 188 protein–ligand complexes [34]. AutoDock 4 was launched in a Cygwin interface in the Windows operating system or from ADT in the Linux operating system. Docking logs were analyzed in the graphical user interface of ADT according to the

instructions in the user guide of AutoDock 4. The results were clustered into bins of similar conformations according to the cluster root mean square deviation (rmsd) and orientation. The docked energy is the sum of the intermolecular and the internal energies. For a representative docking instance, the orientation or pose with the lowest estimated free energy (ΔG) of binding (docked energy + torsional free energy – unbound system's free energy) was chosen in each cluster.

2.4. Flex–rigid versus flex–flex docking

One of the novel features of AutoDock 4 allows side chains in the protein as well as in the ligand to be flexible. For the docking studies reported in this paper a single bond between C^{δ} and $N^{\varepsilon}H$ in Arg301 is flexible and hence this protocol is termed flex–flex docking. This variable torsion resulted in more favorable docking instances as determined by the scoring function than those in flex–rigid docking where all of the protein side chains are rigid. The guanidino group of Arg301 and the amide NH of Gly322 function to polarize the carbonyl of the D-alanyl phosphate intermediate for nucleophilic attack by the amino group of D-alanine or by the alkoxide group of D-lactate [17]. Thus, while the crystallographic structure shows that Arg301 functions in polarizing the carbonyl in D-alanyl phosphate in the oxyanion hole, it is proposed that the guanidino group dynamically orients to provide dual functionality, i.e. in substrate orientation as well as stabilizing the transition state. To study this process, docking orientations are compared in flex–rigid and flex–flex dockings.

3. Results

3.1. Docking poses of D-lactate in subsite 2

Two clusters of D-lactate dockings (A and B) were compared and poses with the lowest ΔG of binding in each cluster are shown in Fig. 2. In flex–flex docking (see Section 2) the A cluster adopts an orientation in which the guanidino group of Arg301 (11.7°, C^{γ}–C^{δ}–N^{ε}–H) promotes bifurcated H-bonding of the D-lactate hydroxyl whereas the B cluster adopts an orientation that does not involve H-bonding between D-lactate and this arginine side chain. In cluster B, the orientation of the guanidino group (52.8°, C^{γ}–C^{δ}–N^{ε}–H) is similar to that determined in the crystallographic measurements (49.2°) of the phosphorylated analog **2** [17]. The second feature of the A cluster is the H-bond between the D-lactate hydroxyl and the phospho ester of the D-alanyl phosphate intermediate in subsite 1. This H-bond is not observed in the B cluster of dockings. The distances (Fig. 1: D1–5) described in the crystal structure of phosphoryl-phosphinate **2**-ligase were measured for the docking poses of clusters A and B (Table 1). The increase of distance D5 in cluster A reflects the change in orientation (0.8 Å) of the guanidino group of Arg301. With the exception of D4, the distances for pose B are significantly larger than those observed in pose A. Not only do the distances D1–D4 of pose A correlate well with the measurements of the co-crystallized phosphoryl-phosphinate **2**-ligase, but the nucleophile–electrophile proximity in pose A (O → C) is 3.1 Å. This is much shorter than that observed for pose B (6.5 Å). The sum of the van der Waals radii of these atoms is 3.2 Å. Thus, the orientation found in pose A has three H-bonds for assisting in nucleophile activation in addition to a close nucleophile–electrophile orientation.

3.2. Docking poses of D-alanine in subsite 2

The orientation of D-alanine in subsite 2 would not be expected to show that of D-lactate in cluster A with the bifurcated H-bond from Arg301. For D-alanine docking, the same flex–flex protocol as that for D-lactate was used. In Fig. 2, two clusters, C and D, of D-alanine docking instances were observed and the poses with the lowest ΔG were also compared with distances in the phosphoryl-phosphinate **2**-ligase (Table 1). In pose C, D4 agrees well with that determined in the co-crystallographic structure. However, D1, D2 and D3 are 1.9, 2.2, and 1.4 times that observed for the corresponding distances in ligase-**2**. The nucleophile–electrophile distance (N → C, 3.2 Å) is almost identical to that observed for D-lactate in pose A (3.1 Å). While the values of ΔG for the C and D poses are almost identical (Table 2), the orientation of those in cluster D correlate poorly with the distances observed for ligase-**2** (Table 1).

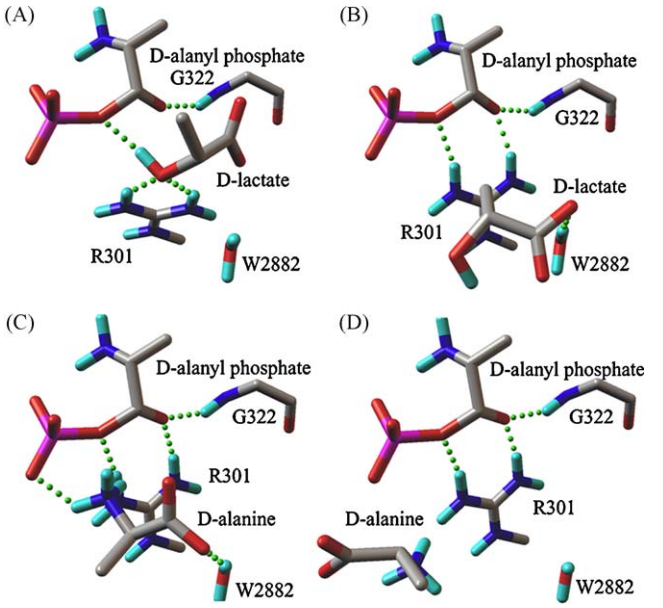

Fig. 2. Docking poses of D-lactate (A and B) and D-alanine (C and D) in subsite 2. Two flex–flex docking protocols, one with D-lactate and one with D-alanine, were run in AutoDock 4. Orientations in each cluster with the lowest ΔG are shown. In cluster A, 44/150 (29%) (rmsd = 0.27) docking instances cluster in an orientation of D-lactate that involves H-bonding of D-lactate to the guanidino of Arg301. In cluster B, 104/150 (69%) (rmsd = 0.35) docking instances cluster in an orientation that involves H-bonding to W2882. In the second protocol with D-alanine, cluster C includes 94/150 (62%) (rmsd = 0.19) and cluster D includes 56/150 (37%) (rmsd = 0.43) docking instances in which W2882 plays no role. Each orientation shows the H-bonding of Gly322 to illustrate the polarization of the carbonyl of the D-alanyl-phosphate intermediate on subsite 1. The Mg^{2+} ions are not shown. For stereo views of poses A and C: see Appendix A, S1 and S2, Supplementary data. For CPK models of poses A and B: Appendix A, S3, Supplementary data.

Table 1
Distances (Å) in Subsite 2 for the docking poses of D-lactate and D-alanine.

Distance (Å)[a]	Phosphoryl- phosphinate **2** Ligase[b]	D-Lactate		D-Alanine	
		A	B	C	D
D1	3.5	3.7	5.3	6.7	7.2
D2	2.6	2.9	7.2	5.7	11
D3	4.0	4.0	5.2	5.5	11
D4	2.8	2.9	3.0	2.9	7.6
D5	3.0	3.8	3.0	3.1	3.0
O → C[c]	–[d]	3.1	6.5	–	–
N → C[c]	–[d]	–	–	3.2	5.5

[a] Distances were measured on the pose in flex-flex docking with the lowest ΔG in each cluster (Fig. 2, A-D). See Fig. 1 for schematic.
[b] D1–D5 were calculated from the coordinates of the co-crystallized phosphoryl phosphinate **2** –ligase [17].
[c] The O → C and N → C distances represent those between the nucleophile R–O: of D-lactate or R–NH_2: of D-alanine and the electrophilic carbonyl carbon of the D-alanyl phosphate in subsite 1.
[d] Not relevant.

Table 2
The estimated ΔG of binding for the docking poses.

		ΔG (kcal/mol)
D-Lactate		
Flex–flex	A[a]	−6.0
Flex–flex	B[a]	−6.0
Flex–rigid	–[b]	−1.4
D-Alanine		
Flex–flex	C[a]	−9.4
Flex–flex	D[a]	−9.2
Flex–rigid	–[b]	−3.7

[a] The lowest energy pose in flex–flex docking is used to calculate the estimated ΔG of binding. These are shown in Fig. 2A–D.
[b] The lowest energy poses in flex–rigid docking are from Fig. 4.

In contrast to the cluster A docking instances with D-lactate, those in cluster C of D-alanine do not appear to show the dynamic orientation of the guanidino group of Arg301 (D5 = 3.1 Å) that was observed in the flex–flex docking of D-lactate. This observation implies either that the guanidino group remained stationary during the flex–flex docking, or that the final docking instances have not reflected the dynamic orientation of this group in facilitating D-alanine docking. To distinguish between these possibilities, the number of energy evaluations in the flex–flex docking protocol was reduced from 5 million to 500. Under this condition, the docking files for D-alanine were examined for instances in which the guanidino group rotates in order to facilitate the docking of D-alanine. Such a docking instance is shown in Fig. 3. While the docking orientation of D-alanine is similar to that in cluster C, the guanidino group shows a torsion (C^{γ}–C^{δ}–N^{ε}–H) of 9.1° similar to that observed in cluster A for D-lactate. Thus, it is concluded that docking of D-alanine also involves the flexibility of the Arg301 guanidino group.

3.3. Flex–rigid versus flex–flex dockings of D-alanine and D-lactate

Flex–rigid dockings of D-lactate and D-alanine were compared with the results of the flex–flex docking protocols described above to define further the role of the guanidino side chain of Arg301. In the case of D-lactate (Fig. 4, D-lactate), the ΔG of binding is −1.4 kcal/mol in flex–rigid docking (Table 2). The bifurcated H-bond with Arg301 observed in flex–flex docking is not observed. For D-alanine the estimated ΔG of binding is −3.7 kcal/mol (Table 2) for the single cluster (Fig. 4, D-alanine). In flex–flex docking (Fig. 2, pose C) the minimum energy pose is −9.4 kcal/mol (Table 2). Thus, comparison of flex–rigid docking with flex–flex docking further illustrates the importance that dynamic orientation of the Arg301 guanidino group plays in positioning the acceptor ligands, D-lactate or D-alanine, in subsite 2.

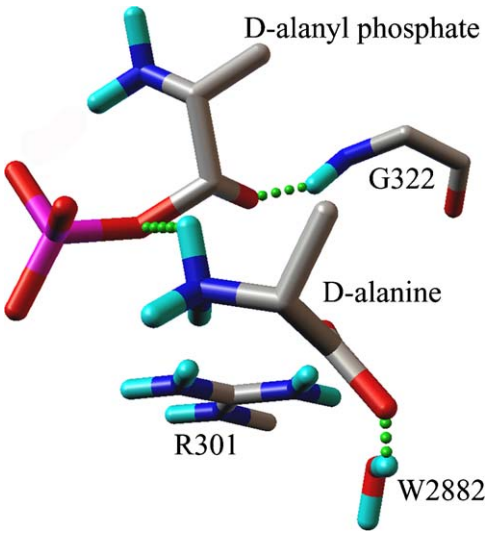

Fig. 3. One pose of D-alanine in the flex–flex docking protocol using reduced energy evaluations. The number of evaluations was reduced from 5 million to 500. (For interpretation of the references to color in this figure legend, the reader is referred to the web version of the article.)

3.4. Chiral specificity of lactate and alanine dockings

While the L-isomer of lactate is not a substrate for the ligase, docking studies reveal that this isomer does in fact dock to the enzyme using the bifurcated H-bonding of Arg301 (Fig. 5). However, in contrast to the D-isomer, this orientation utilizes H-bonding of the lactate hydroxyl to W2882 instead of H-bonding to the phospho ester of D-alanyl phosphate. Thus, the orientation of the L-isomer positions the potential nucleophile away from the electrophilic carbonyl of the D-alanyl phosphate. Studies with L-alanine provided no convergence of the docking instances and hence no meaningful orientation was observed.

3.5. Role of W2882 in the docking of D-lactate and D-alanine

One of the key components of subsite 2 is W2882. It forms a bridge between the carboxylate oxygen atom of **2** and the backbone amide of Leu328. In order to define the importance of the water molecule in this subsite, the docking protocols, one with D-lactate and one with D-alanine, were performed without this molecule. As shown in Fig. 6, orientations of the two substrates, position the nucleophile 5.8 Å (D-lactate) and 5.3 Å (D-alanine) from the electrophilic carbonyl of D-alanyl phosphate. Clearly,

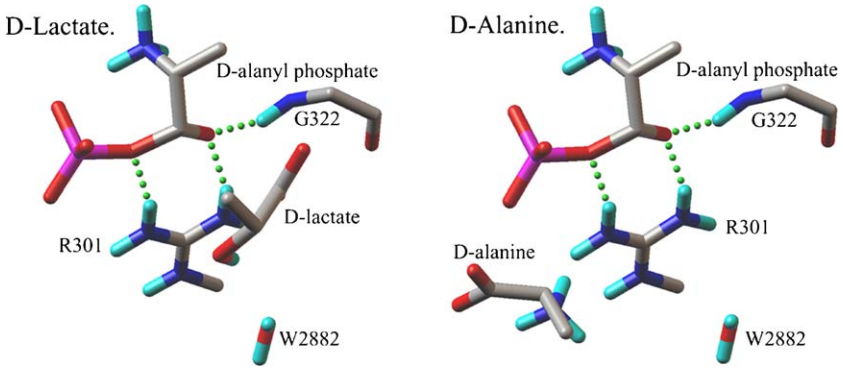

Fig. 4. Orientations of D-lactate and D-alanine in flex–rigid docking. For the flex–rigid docking of D-lactate (143/150, rmsd = 0.30 Å) and D-alanine (147/150, rmsd = 0.58 Å), single clusters were observed. A pose with the lowest estimated ΔG of binding is presented. (For interpretation of the references to color in this figure legend, the reader is referred to the web version of the article.)

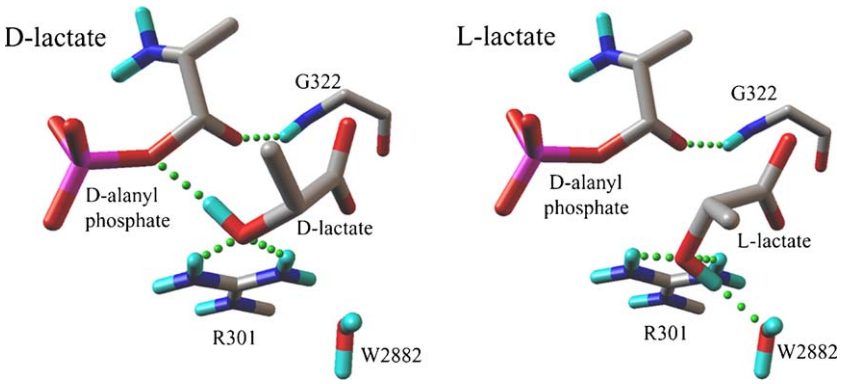

Fig. 5. Chiral specificity in docking D- and L-lactate. For comparison, the docking of D-lactate using the bifurcated H-bonding of Arg301 is shown with H-bonding of the hydroxyl group to the D-alanyl phosphate (left panel). In the right panel, the bifurcated H-bonding of Arg301 with L-lactate positions the hydroxyl group for H-bonding with W2882. (For interpretation of the references to color in this figure legend, the reader is referred to the web version of the article.)

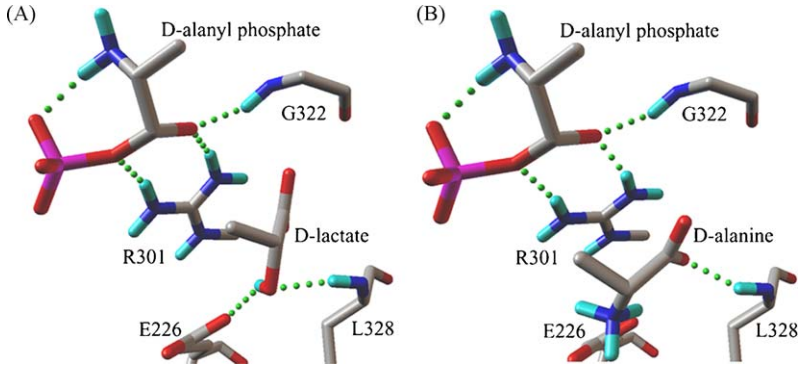

Fig. 6. Role of W2882 in the docking of D-lactate (A) and D-alanine (B). W2882 was deleted from the protein file used for the flex–flex dockings in Fig. 2. In A, a single cluster (rmsd = 0.45) of 150 dockings was observed while in B a single cluster (rmsd = 0.26) of 150 dockings was observed. (For interpretation of the references to color in this figure legend, the reader is referred to the web version of the article.)

these orientations appear to be unproductive when compared to the docking poses shown in Fig. 2, A and C, where W2882 is present.

4. Discussion

The molecular docking studies suggest that the orientation of D-lactate in subsite 2 is determined by bifurcated H-bonding with the guanidino side chain of Arg301. This orientation together with H-bonding of the hydroxyl to the phospho ester of D-alanyl phosphate may provide a mechanism of nucleophile activation (R–O:) for D-lactate. This orientation positions the nucleophile within 3.1 Å of the carbonyl-carbon of the D-alanyl phosphate as well as providing a mechanism of deprotonation for the synthesis of the depsipeptide, D-ala-D-lactate. D-Alanine, on the other hand, assumes a different orientation but one which also brings the nucleophile ($R–NH_2$:) to within 3.2 Å of the electrophilic carbonyl of the D-alanyl phosphate. To activate this nucleophile, deprotonation of the amino group may be accomplished by transfer of the proton to the leaving phosphate group of D-alanyl phosphate. This suggestion is supported by the H-bonding of the protonated amino group of the zwitterion to this phosphate intermediate. Each of the docking orientations, cluster A and cluster C (Fig. 2.), brings the D-lactate and D-alanine to within van der Waals contact for nucleophilic attack.

It may be argued that the docking experiments presented in this paper represent features of artificial docking. These include: (a) the proposed dual functionality of the guanidino group (Arg301) and (b) the deletion of the Ω-loop and serine–serine loop (see below).

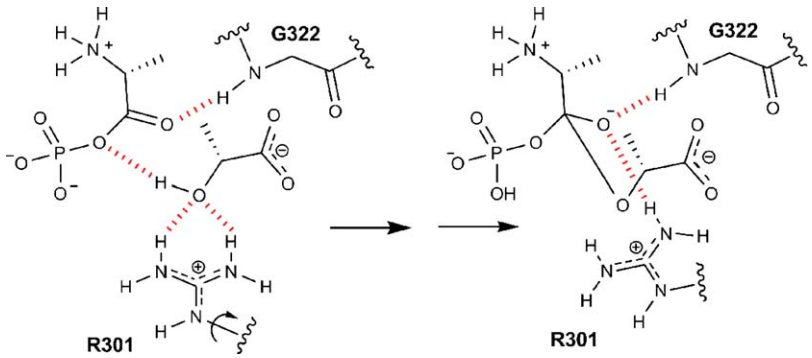

Fig. 7. Role of Arg301 in nucleophile activation of D-lactate (left panel) and stabilization of the transition state (right panel). H-bonds are highlighted in red. (For interpretation of the references to color in this figure legend, the reader is referred to the web version of the article.)

Each of these could compromise the interpretation of the docking results. Arg301 from the *L. mesenteroides* ligase is strictly conserved in each of the homologs examined [4,15]. This residue along with Gly322 defines the oxyanion hole required for stabilizing the transition state and for generating the electrophilic center in the ligation reaction. There is a concern whether the guanidino group of Arg301 has dual functionality, i.e. stabilize the transition-state intermediate and function in nucleophile activation of D-lactate. To address this concern, a sequential two-stage process for D-lactate utilization is proposed (Fig. 7). In the first, nucleophile activation (R–O:) is facilitated by the bifurcated H-bonding of the guanidino group of Arg301 and H-bonding to the D-alanyl phosphate intermediate. In the second stage, the guanidino group orients for H-bonding in the oxyanion hole to stabilize the transition state. Thus, in this sequential mechanism the guanidino group serves two functions: (1) nucleophile activation, and (2) stabilization of the transition state. On the basis of mutagenesis and kinetic arguments, Yun et al. [41] concluded that an essential Arg residue of malonamidase which stabilizes the transition-state oxyanion also plays a primary role in binding of the substrate. This dual functionality of the guanidino side chain is a suggestion similar to that developed for the ligase.

Without removal of the Ω-loop and serine–serine loop, the genetic algorithm of AutoDock 4 is unable to gain access for the ligand to subsite 2. The Ω-loop contains a key residue (Phe261) for determining the specificity of depsipeptide formation [6]. Mutagenesis of F261Y shows a complete loss of D-ala-D-lactate formation [7]. The converse experiment with the ligase from *Escherichia coli* (Y216F) results in a gain of depsipeptide formation [13]. Thus, it was concluded that Phe261, located in the Ω-loop, is a "molecular indicator of D-ala-D-lactate formation" [6]. It was further proposed that the Ω-loop bearing Phe261, together with the serine–serine loop, open and close in each catalytic cycle to let products leave and substrates enter. This substrate-induced conformational change results in significant movements of domain 2 relative to domain 3 and the ordering of the Ω-loop [15,17]. Without the Ω-loop (residues 247–267) the ligase lacks a key residue that plays a role in the binding specificity of D-lactate in subsite 2. However, deletion of this residue together with the Ω-loop does not preclude a study of Arg301 functions as well as other residues that determine subsite 2 specificity. Thus, while the specificity constraints of this subsite may have been modified, the catalytic architecture appears to be intact.

Using a molecular dynamics simulation (CHARMM) of the D-alanine:D-alanine ligase B from *E. coli*, Carlson et al. [36] modeled D-alanyl phosphate in subsite 1 and D-alanine in subsite 2. From electrostatic calculations, it was determined that the D-alanine in subsite 2 is zwitterionic. In comparisons with the VanA ligase it was also concluded that the specificity of binding D-lactate over D-alanine may arise from a difference in ionization characteristics of the two ligands.

Dynamic measurements of the Arg301 guanidino group together with other key residues in subsite 2 may be required to evaluate more fully the function(s) that this side chain plays in the ligation reaction. Since it has not been possible to co-crystallize the *L. mesenteroides* ligase with either D-alanine or D-lactate together with ATP and Mg^{2+}, the docking studies described in this paper may be one of the few methods for defining substrate orientation in this subsite. In addition, these studies may yield insights into the rational design of inhibitors that utilize both the architecture of this subsite as well as ligand orientations.

Acknowledgments

The author thanks Peter Reilly and Luis Petersen, Iowa State University, for their encouragement in this endeavor. I also thank my colleagues Haitao (Mark) Ji, Alfonso Mondragón, Ishwar Radhakrishnan, and Tai Te Wu for many consultations. I am indebted to James Knox, University of Connecticut, for providing essential key recommendations and cautions for these docking experiments. Finally, without the major help and consultation from Jason Pattie, IT Consultant Associate at Northwestern University, the use of AutoDock 4 would have been impossible for the author.

Appendix A. Supplementary data

Supplementary data associated with this article can be found, in the online version, at doi:10.1016/j.jmgm.2010.01.010.

References

[1] F.C. Neuhaus, The enzymatic synthesis of D-alanyl-D-alanine. I. Purification and properties of a D-alanyl-D-alanine synthetase, J. Biol. Chem. 237 (1962) 778–786.
[2] E. Ito, J.L. Strominger, Enzymatic synthesis of the peptide in bacterial uridine nucleotides. II. Enzymatic synthesis and addition of D-alanyl-D-alanine, J. Biol. Chem. 237 (1962) 2696–2703.
[3] C.T. Walsh, Enzymes in the D-alanine branch of bacterial cell wall peptidoglycan assembly, J. Biol. Chem. 264 (1989) 2393–2396.
[4] S. Evers, B. Casadewall, M. Charles, S. Dutka-Malen, M. Galimand, P. Courvalin, Evolution of structure and substrate specificity in D-alanine:D-alanine ligases and related enzymes, J. Mol. Evol. 42 (1996) 706–712.
[5] I.A.D. Lessard, V.L. Healy, I.-S. Park, C.T. Walsh, Determinants for differential effects on D-Ala-D-lactate vs D-Ala-D-Ala formation by the vanA ligase from vancomycin-resistant enterococci, Biochemistry 38 (1999) 14006–14022.
[6] V.L. Healy, I.A.D. Lessard, D.I. Roper, J.R. Knox, C.T. Walsh, Vancomycin resistance in enterococci: reprogramming of the D-Ala-D-Ala ligases in bacterial peptidoglycan biosynthesis, Chem. Biol. 7 (2000) R109–R119.
[7] I.-S. Park, C.T. Walsh, D-Alanyl-D-lactate and D-alanyl-D-alanine synthesis by D-alanyl-D-alanine ligase from vancomycin-resistant *Leuconostoc mesenteroides*. Effects of a phenylalanine 261 to tyrosine mutation, J. Biol. Chem. 272 (1997) 9210–9214.
[8] D. Billot-Klein, L. Gutmann, S. Sable, E. Guittet, J. van Heijenoort, Modification of peptidoglycan precursors is a common feature of the low-level vancomycin-resistant VANB-type *Enterococcus* D366 and of the naturally glycopeptide-resistant species *Lactobacillus casei*, *Pediococcus pentosaceus*, *Leuconostoc mesenteroides*, and *Enterococcus gallinarum*, J. Bacteriol. 176 (1994) 2398–2405.
[9] S. Handwerger, M.J. Pucci, K.J. Volk, J. Liu, M.S. Lee, Vancomycin-resistant *Leuconostoc mesenteroides* and *Lactobacillus casei* synthesize cytoplasmic peptidoglycan precursors that terminate in lactate, J. Bacteriol. 176 (1994) 260–264.
[10] F.C. Neuhaus, The enzymatic synthesis of D-alanyl-D-alanine. II. Kinetic studies on D-alanyl-D-alanine synthesis, J. Biol. Chem. 237 (1962) 3128–3135.
[11] F.C. Neuhaus, J.L. Lynch, The enzymatic synthesis of D-alanyl-D-alanine. III. On the inhibition of D-alanyl-D-alanine synthetase by the antibiotic D-cycloserine, Biochemistry 3 (1964) 471–480.
[12] L.S. Mullins, L.E. Zawadske, C.T. Walsh, F.M. Raushel, Kinetic evidence for the formation of D-alanyl phosphate in the mechanism of D-alanyl-D-alanine ligase, J. Biol. Chem. 265 (1990) 8993–8998.
[13] I.-S. Park, C.-H. Lin, C.T. Walsh, Gain of D-alanyl-D-lactate or D-lactyl-D-alanine synthetase activities in three active site mutants of the *Escherichia coli* D-alanyl-D-alanine ligase B, Biochemistry 35 (1996) 10464–10471.
[14] Y. Shi, C.T. Walsh, Active site mapping of *Escherichia coli* D-Ala-D-Ala ligase by structure-based mutagenesis, Biochemistry 34 (1995) 2768–2776.
[15] S. Liu, J.S. Chang, J.T. Herberg, M.-M. Horng, P.K. Tomich, A.H. Lin, K.R. Marotti, Allosteric inhibition of *Staphylococcus aureus* D-alanine:D-alanine ligase revealed by crystallographic studies, Proc. Natl. Acad. Sci. U.S.A. 103 (2006) 15178–15183.
[16] C. Fan, P.C. Moews, C.T. Walsh, J.R. Knox, Vancomycin resistance: structure of D-alanine:D-alanine ligase at 2.3 Å resolution, Science 266 (1994) 439–443.
[17] A.P. Kuzin, T. Sun, J. Jorczak-Baillass, V.L. Healy, C.T. Walsh, J.R. Knox, Enzymes of vancomycin resistance: the structure of D-alanine-D-lactate ligase of naturally resistant *Leuconostoc mesenteroides*, Structure 8 (2000) 463–470.
[18] J.H. Lee, Y. Na, H.-E. Song, D. Kim, B.-H. Park, S.-H. Rho, Y.J. Im, M.-K. Kim, G.B. Kang, D.-S. Lee, S.H. Eom, Crystal structure of the apo form of D-alanine:D-alanine ligase (Ddl) from *Thermus caldophilus*: a basis for the substrate-induced conformational changes, Proteins: Struct. Funct. Bioinform. 64 (2006) 1078–1082.
[19] D.I. Roper, T. Huyton, A. Vagin, G. Dodson, The molecular basis of vancomycin resistance in clinically relevant enterococci: crystal structure of D-alanyl-D-lactate ligase (VanA), Proc. Natl. Acad. Sci. U.S.A. 97 (2000) 8921–8925.
[20] D. Wu, L. Zhang, Y. Kong, J. Du, S. Chen, J. Chen, J. Ding, H. Jiang, X. Shen, Enzymatic characterization and crystal structure analysis of the D-alanine-D-alanine ligase from *Helicobacter pylori*, Proteins 72 (2008) 1148–1160.
[21] M. Prévost, D. Van Belle, P.M. Tulkens, P. Courvalin, F. Van Bambeke, Modeling of *Enterococcus faecalis* D-alanine:D-alanine ligase: structure-based study of the active site in the wild-type enzyme and in glycopeptide-dependent mutants, J. Mol. Microbiol. Biotechnol. 2 (2000) 321–330.
[22] T.D.H. Bugg, G.D. Wright, S. Dutka-Malen, M. Arthur, P. Courvalin, C.T. Walsh, Molecular basis for vancomycin resistance in *Enterococcus faecium*BM4147:

biosynthesis of a depsipeptide peptidoglycan precursor by vancomycin resistance proteins VanH and VanA, Biochemistry 30 (1991) 10408–10415.
[23] W.P. Hammes, F.C. Neuhaus, On the mechanism of action of vancomycin: inhibition of peptidoglycan synthesis in *Gaffkya homari*, Antimicrob. Agents Chemother. 6 (1974) 722–728.
[24] L.S. Johnston, F.C. Neuhaus, Initial membrane reaction in the biosynthesis of peptidoglycan. Spin-labeled intermediates as receptors for vancomycin and ristocetin, Biochemistry 14 (1977) 2754–2760.
[25] M. Arthur, P. Reynolds, P. Courvalin, Glycopeptide resistance in enterococci, Trends Microbiol. 4 (1996) 401–407.
[26] T.D.H. Bugg, S. Dutka-Malen, M. Arthur, P. Courvalin, C.T. Walsh, Identification of vancomycin resistance protein VanA as a D-alanine:D-alanine ligase of altered substrate specificity. Glycopeptide resistance in enterococci, Biochemistry 30 (1991) 2017–2021.
[27] P. Courvalin, Vancomycin resistance in gram-positive cocci, Clin. Infect. Dis. 42 (2006) S25–34.
[28] G.D. Wright, C.T. Walsh, D-Alanyl-D-alanine ligases and the molecular mechanism of vancomycin resistance, Acc. Chem. Res. 25 (1992) 468–473.
[29] A. Kovač, J. Konc, B. Vehar, J. Bostock, I. Chopra, D. Janežič, S. Gobec, Discovery of new inhibitors of D-alanine:D-alanine ligase by structure based virtual screening, J. Med. Chem. 51 (2008) 7442–7448.
[30] B.A. Ellsworth, N.J. Tom, P.A. Bartlett, Synthesis and evaluation of inhibitors of bacterial D-alanine:D-alanine ligases, Chem. Biol. 3 (1996) 37–44.
[31] P.K. Chakravarty, W.J. Greenlee, W.H. Parsons, A.A. Patchett, P. Combs, A. Roth, R.D. Busch, T.N. Mellin, 3-Amino-(2-oxoalkyl)phosphonic acids and their analogues as novel inhibitors of D-alanine:D-alanine ligase, J. Med. Chem. 32 (1989) 1886–1890.
[32] A.M. Lacoste, A.M. Chollet-Gravey, L. Vo Quang, Y. Vo Quang, F. Le Goffic, Time-dependent inhibition of *Streptococcus faecalis* D-alanine:D-alanine ligase by α-aminophosphonamidic acids, Eur. J. Med. Chem. 26 (1991) 255–260.
[33] W.H. Parsons, A.A. Patchett, et al., Phosphinic acid inhibitors of D-alanyl-D-alanine ligase, J. Med. Chem. 31 (1988) 1772–1778.
[34] R. Huey, G.M. Morris, A.J. Olson, D.S. Goodsell, A semiempirical free energy force field with charge-based desolvation, J. Comput. Chem. 28 (2007) 1145–1152.
[35] G.M. Morris, R. Huey, W. Lindstrom, M.F. Sanner, R.K. Belew, D.S. Goodsell, A.J. Olson, AutoDock 4 and AutoDockTools 4: automated docking with selective receptor flexibility, J. Comput. Chem. 30 (2009) 2785–2789.
[36] H.A. Carlson, J.M. Briggs, J.A. McCammon, Calculation of the pK_a values for the ligands and side chains of *Escherichia coli* D-alanine:D-alanine ligase, J. Med. Chem. 42 (1999) 109–117.
[37] N. Guex, M.C. Peitsch, SWISS-MODEL and the Swiss-PdbViewer: an environment for comparative protein modeling, Electrophoresis 18 (1997) 2714–2723.
[38] D. Chen, M. Misra, L. Sower, J.W. Peterson, G.E. Kellogg, C.H. Schein, Novel inhibitors of anthrax edema factor, Bioorg. Med. Chem. 16 (2008) 7225–7233.
[39] J. Gasteiger, M. Marsili, Iterative partial equalization of orbital electronegativity—a rapid access to atomic charges, Tetrahedron 36 (1980) 3219–3228.
[40] M.F. Sanner, Python: a programming language for software integration and development, J. Mol. Graph. Mod. 17 (1999) 57–61.
[41] Y-.S. Yun, W. Lee, S. Shin, B.-H. Oh, K.Y. Choi, Arg-158 is critical in both binding the substrate and stabilizing the transition-state oxyanion for the enzymatic reaction of malonamidase E2, J. Biol. Chem. 281 (2006) 40057–40064.